

# Contaminant Mass Transfer from NAPLs to Water Studied in a Continuously Stirred Flow-Through Reactor

Lihua Liu<sup>1</sup>; Uli Maier<sup>2</sup>; Peter Grathwohl<sup>3</sup>; and Stefan B. Haderlein<sup>4</sup>

**Abstract:** The release of nonaqueous-phase liquids (NAPLs) from porous media to groundwater is a widespread environmental problem. The mass transfer of individual NAPL components controls both the extent of groundwater contamination and the persistence of the residual NAPL phase. In order to quantify this key process, small-scale experimental studies on NAPL-water mass transfer were performed in a dynamic system mimicking environmental conditions with “clean” water continuously flowing through the NAPL pool. To describe this process, a modified simulation method was developed and validated by the experimental data. The experimental system consisted of a custom-designed flow cell (with NAPL and water) connected to the peripheral equipment (e.g., pump, water source). This continuously stirred flow-through reactor was used to perform mass transfer experiments with simple and complex model NAPL–water systems. To simulate the experimental data (concentration versus time profiles of individual NAPL compounds), an analytical solution of a standard mass transfer model was adapted in simple model NAPL systems, and a numerical method was employed for complex multicomponent model NAPL–water systems containing phenols, heteroaromatic compounds, and polycyclic aromatic hydrocarbons (PAHs). The numerical model was developed based on a mass balance equation and a general form of Raoult’s law. The simulated concentration profiles of the various solutes matched well the experimental data only if the nonideal behavior of the more polar solutes was accounted for. Using the developed numerical model simulated mass transfer coefficients for individual NAPL components compared well with previously published values if available. DOI: 10.1061/(ASCE)EE.1943-7870.0000528. © 2012 American Society of Civil Engineers.

**CE Database subject headings:** Mass transfer; Coefficients; Fuels; Groundwater pollution; Porous media.

**Author keywords:** Mass transfer coefficients; NAPL-water interphase; Fuel derived contaminants; Groundwater contamination.

## Introduction

Aquifers and soils in industrialized areas are often contaminated by nonaqueous phase liquids (NAPLs), which are long-term sources of groundwater plumes (Eberhardt et al. 2002; Heyse et al. 2002; Luthy et al. 1994; Powers et al. 1991). As groundwater flows passed trapped NAPL ganglia or pools, a fraction of the NAPL dissolves in the aqueous phase and creates a dissolved plume of hydrocarbons. The distribution of the solutes between the NAPL and the aqueous phase is governed by the hydrodynamic conditions and the molecular diffusion of solutes in both the phases and the interphases. The kinetics of solute dissolution from NAPLs has been extensively studied, and several mass transfer models derived theoretically and empirically have been previously published (Ahn and Lee 1990; Alshafie and Ghoshal 2004; Benhabib et al. 2006;

Cho et al. 2005; Chrysikopoulos et al. 2003; Ghoshal et al. 2004; Lee 2004; Lee et al. 2007; Mukherji et al. 1997; Ramaswami et al. 1997; Ramaswami and Luthy 1997; Schluep et al. 2001). Critical reviews of recent work on NAPL dissolution in porous media have indicated that the most promising research progress, in addition to exploitation of combined large-scale field and computational investigations (Broholm et al. 2005), may be determined by the clarification of the role of nonideal NAPL mixtures and identification of intra-NAPL mass transfer processes (Khachikian and Harmon 2000). Most existing models were established based on the assumption that mass transfer rates inside the NAPL are faster than the dispersive transport from the interface, i.e., the aqueous boundary layer governs the dissolution process. A few studies have suggested that slow diffusion of solutes within the NAPL or at the NAPL-side boundary layer of the interface may also limit rates of mass transfer (Ghoshal et al. 2004; Ortiz et al. 1999). Furthermore, a visible external boundary forming gradually at the NAPL–water interface was observed in some studies (Alshafie and Ghoshal 2004; Barranco and Dawson 1999; Ghoshal et al. 2004; Liu et al. 2009; Luthy et al. 1993; Mukherji et al. 1997). Ortiz et al. (1999) demonstrated that the mass transfer of polycyclic aromatic hydrocarbons (PAHs) is a dynamic process and is affected by the concomitant viscosity increase in the NAPL. The mass transfer coefficient,  $k$ , (in units of  $\text{cm s}^{-1}$ ) is the reciprocal of the resistance to mass transfer and involves molecular and advective transport of solutes within the physical systems. For single and multicomponent NAPL dissolution systems, the mass transfer coefficient is a function of several dependent factors and generally a “variable” rather than a constant (Kim and Chrysikopoulos 1999; Chrysikopoulos and Kim 2000). An estimation of the mass transfer coefficient has been proposed involving parameters such as water velocity, NAPL saturation, interfacial areas, NAPL composition,

<sup>1</sup>Associate Professor, Guangzhou Institute of Energy Conversion, Chinese Academy of Sciences, No. 2 Nengyuan R., Wushan, Tianhe District, Guangzhou 510640, China (corresponding author). E-mail: liulh@ms.giec.ac.cn

<sup>2</sup>Research Scientist, Univ. of Tübingen, Dept. of Geosciences, Hölderlinstraße 12, D-72076 Tübingen, Germany. E-mail: uli.maier@uni-tuebingen.de

<sup>3</sup>Professor, Univ. of Tübingen, Dept. of Geosciences, Hölderlinstraße, D-72076 Tübingen, Germany. E-mail: grathwohl@uni-tuebingen.de

<sup>4</sup>Professor, Univ. of Tübingen, Center for Applied Geosciences, Hölderlinstraße 12, D-72076 Tübingen, Germany. E-mail: haderlein@uni-tuebingen.de

Note. This manuscript was submitted on May 5, 2011; approved on December 22, 2011; published online on July 16, 2012. Discussion period open until January 1, 2013; separate discussions must be submitted for individual papers. This paper is part of the *Journal of Environmental Engineering*, Vol. 138, No. 8, August 1, 2012. ©ASCE, ISSN 0733-9372/2012/8-826–832/\$25.00.

and grain-size of the porous medium (Brusseau et al. 1997; Ortiz et al. 1999; Powers et al. 1992; Powers et al. 1991; Chrysikopoulos et al. 2003). Previous researchers, however, either studied NAPLs as one material (Ghoshal and Luthy 1998) or focused on one or more components. These components, mostly PAHs and/or benzene, toluene, ethylbenzene, and xylene (BTEX), had similar molecular structures, physicochemical properties, behaviors, and experimental or analytical constraints. In these previous studies, the ideal Raoult's law was generally assumed to be valid. There is no research reported about the mass transfer behavior of compound groups exhibiting very different polarities and thus different intermolecular interactions within one NAPL system, although such compounds, e.g., PAHs and phenols, always coexist in real NAPLs. This study is motivated by the lack of understanding of the effects of molecular structure and distinctly different physicochemical properties on mass transfer rates, as well as the applicability of Raoult's law for such complex systems.

The main objectives of this work are (1) to design a versatile experimental set-up to determine mass transfer coefficients under different hydromechanical and physicochemical conditions, (2) to test the applicability of Raoult's law for complex NAPL mixtures, and (3) to establish a numerical model that describes the mass transfer process and quantifies the related parameters.

## Materials and Methods

### Materials-Model NAPLs

The present work is based on synthetic single compound or multi-compound NAPLs rather than real NAPLs to minimize the effect of solid particles and high molecular weight compounds such as asphaltenes and resins. These solid particles and high molecular weight compounds are believed to contribute to the formation of viscous interfacial phases ("skins") and impede the mass transfer process (Andersen et al. 2001; Barranco and Dawson 1999; Jeribi et al. 2002; Sullivan and Kilpatrick 2002; Zheng and Powers 2003).

In the single-solute experiments, phenanthrene was used as the probe compound in the NAPL phase at a concentration of 3 g in 250 mL toluene. This concentration ( $12 \text{ g L}^{-1}$ ) represents that of most real NAPLs, e.g., coal tar and creosotes (Eberhardt 2002; Mahjoub et al. 2000; Nelson et al. 1996; Tiruta-Barna et al. 2006). The single-solute NAPL was used to test and improve the experimental set-up, the sampling procedure, and the analytical methods, as well as for validating the numerical model for multi-component NAPLs. Toluene was chosen as the bulk component of the NAPL because its solubility properties are versatile for organic

compounds and because of its aromatic nature (Mahjoub et al. 2000; Peters et al. 1997).

The multicomponent model NAPL was comprised of seven solutes dissolved in toluene. The solutes were naphthalene (98%; Aldrich), phenanthrene (98%; Alfa Aesar), 2,3-benzofuran (99%; Aldrich), phenol (99.5%; Fluka), m-cresol (99%; Aldrich), 1-naphthol (99%; Aldrich), and phenoxathiin (98%; Alfa Aesar). These solutes represent the most frequently detected groundwater contaminants, which include PAHs, phenols, and heterocyclic aromatic compounds. These contaminants are also major constituents of NAPLs found in the environment, with the exception of phenoxathiin, which has never been detected in the field nor reported in the literature. However, because of its similar molecular structure and physicochemical properties, phenoxathiin was chosen as an alternative to phenanthrene to validate the experimental and modeling procedures. The initial masses and concentrations ( $C_o$ ) of these compounds in the NAPL are listed in Table 1. The aqueous phase consisted of toluene-saturated water to avoid depletion of toluene from the NAPL phase and to keep the volume of NAPL constant.

### Continuously Stirred Flow-through Reactor System

An experimental system was designed and a numerical simulation was developed to study the mass transfer process of multicomponents from a NAPL to the aqueous phase. The dynamic experimental set-up with a custom-made glass cell (500 mL) is shown in Fig. 1. The cell was sealed with a Viton ring and a horse shoe to make it gas tight, and it was filled with a predefined volume ratio (1:1 in this test) of water and NAPL. Even though only a light-NAPL (LNAPL) water system was tested, the reactor could also be used for dense-NAPL (DNAPL) water systems. So far, such dynamic systems have not been described for mass transfer studies of NAPLs. A grooved basket was fixed to the inside cover to hold a stirring bar on the top inside the cell. This allowed magnetic stirring bars to operate at the top and the bottom of the flow-through cell to mix both phases independently. In this work, LNAPLs with low initial solute concentrations were used, therefore only one stirring bar was set at the bottom to mix the aqueous phase. The stirring rate was adjusted carefully to minimize the influence of mechanical force. The cell was fed with toluene-saturated water from a reservoir and was connected to a peristaltic pump (ISMATEC, Switzerland) through stainless steel tubing (1/16", Klaus Ziemer GmbH, Mannheim) to precisely control the flow rate of the aqueous phase. A three-way valve connector (Swagelok 1/16") was used to connect the reactor to the pump and the sampling port. This experimental set-up is quite versatile and can be operated under a wide range of hydromechanical and physicochemical conditions.

**Table 1.** Initial Composition of the Multicomponent Model NAPL

Component	Mass (g)	MW (g/mol)	$S_i$ (mg/L)	$C_o$ (g/L)	Moles	Mole fraction (%)
Phenol	0.00088	94.1	82800 <sup>a</sup>	0.0044	0.000009	0.0005
m-Cresol	0.00094	108.1	22700 <sup>b</sup>	0.0047	0.0000087	0.0005
1-Naphthol	0.0019	144.2	866 <sup>a</sup>	0.0094	0.000013	0.0007
Naphthalene	0.9081	128.2	105.67 <sup>c</sup>	4.54	0.0071	0.38
Phenanthrene	1.993	178.2	4.21 <sup>c</sup>	9.96	0.011	0.60
Phenoxathiin	2.003	200.2	0.449 <sup>a</sup>	10.0	0.010	0.54
2,3-Benzofuran	0.0570	118.1	678 <sup>b</sup>	0.29	0.00048	0.026
Toluene (solvent)	200 mL	92.1	526 <sup>b</sup>	839.7	1.82	98.44

<sup>a</sup>Solid water solubility where subcooled liquid solubility is unavailable.

<sup>b</sup>From the physical properties database (PHYSPROP) <http://www.syrres.com/esc/physprop.htm>.

<sup>c</sup>Subcooled liquid solubility from Peters et al. (1999, 1997).

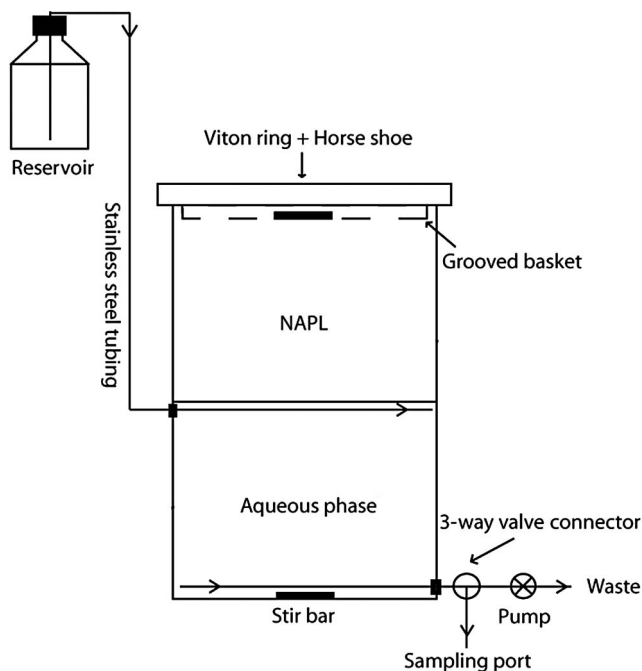


**Fig. 1.** Setup of the continuously stirred flow-through reactor system

The aqueous samples of the effluent were collected and analyzed for their organic solute concentrations.

Preliminary tests were run for 24 h, and after 6 h, steady state conditions were observed with a flow rate of  $0.5 \text{ mL min}^{-1}$ . The average residence time of the water in the reactor was about 8 h, therefore, the subsequent experiments were performed for 8 h ( $0.5 \text{ mL min}^{-1}$ ). The first sample was obtained within 5 min after the NAPL and aqueous phases were in contact. Because a few minutes were needed to seal the cell, it was impossible to take a sample at time zero. The sampling interval was increased to 10 min within the first 2 h, and later extended to 20, 30, and 60 min every hour, resulting in a total of 18 aqueous samples in 8 h.

To test the mass loss due to volatilization during sampling, a vial containing a 5 mL naphthalene solution with a concentration similar to that of the aqueous samples was placed inside the draft cupboard synchronously and sealed after the sampling time period. No change of concentration was detected in the tested samples, and thus the volatilization effect could be neglected.

### Chemical Analyses

Aqueous samples (5 mL) were spiked with 5–10  $\mu\text{L}$  of internal standard (acenaphthylene,  $2 \text{ g L}^{-1}$  in toluene) and extracted by 0.5 to 1.0 mL ethyl acetate. Aliquots of the extracts were analyzed by GC-MS (HP 5890/II with HP 5972 MSD) together with four external standards (mixture of all organic compounds in cyclohexane at four different concentrations).

Analytes were separated using a  $30 \text{ m} \times 0.25 \text{ mm}$  DB-5MS column (J&W Scientific) with  $0.25 \mu\text{m}$  film thickness. The injector temperature was maintained at  $270^\circ\text{C}$  and the injection volume was  $1 \mu\text{L}$ . Helium was used as the carrier gas at a constant flow of  $0.6 \text{ mL/min}$ . The oven temperature program was  $50^\circ\text{C}$  for 2 min, increased at a rate of  $8^\circ\text{C/min}$  to  $90^\circ\text{C}$ , then increased to  $270^\circ\text{C}$  at a rate of  $18^\circ\text{C/min}$ , held for 10 min, and finally raised to  $310^\circ\text{C}$  at a rate of  $10^\circ\text{C/min}$  and held for 6.5 min.

The concentrations of the aqueous samples were calculated according to the slope of a linear calibration and the corresponding area obtained from the mass-spectrometry (MS) signal.

### Modeling Approach

- 1 Dynamic equilibrium process: the mass transfer of solutes from NAPL to water is driven by diffusion and advection. Consequently, the change of the aqueous phase concentrations with respect to time can be described by two terms (Alshafie and Ghoshal 2004; Ghoshal et al. 2004; Luthy et al. 1994)

$$\frac{dC_{i,t}}{dt} = \frac{A}{V_w} k_{i,t} (C_{i,\text{eq},t} - C_{i,t}) - \frac{Q}{V_w} C_{i,t} \quad (1)$$

The first term on the right-hand side is referred to as the diffusive term,  $E$ , between the organic and the aqueous phase. This term also represents the sink to the organic phase. The second term is the advective flux, with  $C_{i,t}$  ( $\mu\text{g mL}^{-1}$ , or  $\mu\text{g L}^{-1}$ ) denoting the time-dependent concentrations of solute  $i$  in the water phase. The term  $C_{i,\text{eq},t}$  is the equilibrium aqueous phase concentration at time  $t$  of the solute  $i$ , and the terms  $A$  ( $\text{cm}^2$ ),  $V_w$  ( $\text{cm}^3$ ), and  $Q$  ( $\text{mL min}^{-1}$ ) are the interfacial area, water volume, and flow rate, respectively. The overall mass transfer coefficient of solute  $i$  is  $k_{i,t}$  ( $\text{cm min}^{-1}$ ). Note that both terms in Eq. (1) have units of mass per volume per time ( $\mu\text{g cm}^{-3} \text{ min}^{-1}$ ). It should also be noted that  $k_i$  is a function of several variables rather than a constant. Therefore, model simulations could yield different results, depending on the system composition and set-up conditions.

- 2 Analytical model: in single solute mass transfer experiments, phenanthrene was used as a probe compound, and the total mass leached from the NAPL phase was less than 0.1% of its initial and remaining mass. The concentration of the solute in NAPL phase  $C_{i,\text{eq},t}$  thus could be treated as a constant. Because the change of NAPL volume and  $k_i$  was considered negligible, integrating Eq. (1) yields

$$C_{i,t} = \frac{A \cdot k_i \cdot C_{i,\text{eq}}}{A \cdot k_i + Q} - \left( \frac{A \cdot k_i \cdot C_{i,\text{eq}}}{A \cdot k_i + Q} - C_{i0} \right) \cdot e^{-[(A/V_w)k_i + Q/V_w](t-t_0)} \quad (2)$$

where  $C_{i0}$  is the solute aqueous concentration at time  $t_0$ . The accuracy of the fit of  $k_i$  for each set of aqueous concentration data was evaluated by the values of the relative residual sum of squares (RRSS), as Eq. (3)

$$\text{RRSS} = \sum_{k=1}^n \left( \frac{C_{i,t} - C'_{i,t}}{C_{i,t}} \right) \quad (3)$$

In this equation,  $C_{i,t}$  is the effluent concentration data point and  $C'_{i,t}$  is the corresponding model prediction.

- 3 Numerical model: in the multicomponent NAPL, highly water soluble compounds such as phenols are significantly depleted from the organic phase during the leaching process. The equilibrium aqueous phase concentrations,  $C_{i,\text{eq},t}$ , decrease significantly with time and thus cannot be treated as a constant. In this case, no analytical solution is available for Eq. (1) and a numerical solution must be adopted. This problem was solved by implementing the general form of Raoult's law

$$C_{i,\text{eq}} = \chi_i \cdot \gamma_i \cdot S_{i,\text{sub}} \quad (4)$$

In Eq. (4),  $\gamma_i$  (–) and  $\chi_i$  (–) are the activity coefficient and the mole fraction of  $i$  in the NAPL, respectively. The value  $S_{i,\text{sub}}$  ( $\mu\text{g mL}^{-1}$ , or  $\mu\text{g L}^{-1}$ ) is the subcooled liquid solubility, meaning the solubility of the compound in a (subcooled) liquid state. Previous research demonstrated that Raoult's law with a

$\gamma_i$  of unity (or very close to unity) holds true for monocyclic and polycyclic aromatic hydrocarbons in both model and real NAPLs (Cline et al. 1991; Eberhardt 2002; Lane and Loehr 1992; Luthy et al. 1993; Chrysikopoulos and Lee 1998). However,  $\gamma_i$  being unity implies a thermodynamically “ideal” solution. For complex NAPLs,  $\gamma_i$  may become a function of the compound’s mole fraction,  $\chi_i$  (Ghoshal et al. 1996; Lee et al. 1998; Lee and Chrysikopoulos 2006). A power law dependence of  $\gamma_i$  on the component  $\chi_i$  ( $\gamma_i = \text{constant } \chi_i^n$ ) is assumed to express the mole fraction dependence. This modifies Eq. (4) to

$$C_{i,\text{eq}} = \alpha_i \cdot \chi_i^{n_i+1} \cdot S_{i,\text{sub}} \quad (5)$$

where  $\alpha_i$  (–) and  $n_i$  (–) denote a mole fraction-independent constant and an empirical exponent of  $\chi_i$ . This exponent should be (1) negative for compounds that may involve strong polar interactions and  $\gamma_i$  decreases with increasing mole fraction, (2) close to zero ( $\gamma_i$  close to 1) for structurally similar components, which is the ideal case, meaning the molecular interactions in the NAPL phase are similar to those in a liquid phase of the pure solute, and (3) positive for the solute and solvent both undergoing additional intermolecular interactions that were unavailable to them in their own pure liquid phases. The aqueous phase concentration,  $C_{i,t}$ , can then be obtained from the iterative formulas below

$$C_{i,\text{eq},t} = \alpha_i \cdot \left( M_i / \sum_{j=1}^m M_j \right)^{n_i+1} \cdot S_{i,\text{sub}} \quad (6)$$

$$E_{i,t} = A \cdot k_i \cdot (C_{i,\text{eq},t} - C_{i,t}) \quad (7)$$

$$M_{i,t} = M_{i,t-1} - \frac{\Delta t}{2} \cdot (E_{i,t} + E_{i,t-1}) \quad (8)$$

$$C_{i,t} = \frac{C_{i,t-1} + \frac{\Delta t}{2V_w} \cdot (A \cdot k_i \cdot C_{i,\text{eq},t-1} + E_{i,t-1} - Q \cdot C_{i,t-1})}{1 + \frac{\Delta t}{2V_w} \cdot (Q + A \cdot k_i)} \quad (9)$$

where  $\Delta t$  (min) = time step;  $m$  (–) = number of compounds;  $M$  (mol) = mass of  $i$  within the organic phase; and  $E$  (mol min<sup>-1</sup>) = exchange term (corresponding to first term on the right-hand side of Eq. (1) in units of mass per time). The values  $M_i$  and  $C_i$  are marked by subscripts ( $t$ ) to account for the current time step and ( $t - 1$ ) for the previous time step.

The model is based on Eq. (1) and was programmed in FORTRAN 90. The nonlinear system was solved numerically by Gauss–Seidel iterations with centered time-weighting over the set of Eqs. (6)–(9) until convergence was achieved. The time step was automatically adjusted to split the time until depletion of the most soluble component into a sufficient number of steps (= 100) until that particular compound is totally depleted. This corresponds to an initial time step of 0.0001 min in the given case. The total elapsed time of the simulation represents the experimental period of 480 min.

## Results and Discussion

### Single-Solute NAPL

Simulation results of the single-solute NAPL depletion experiment are shown in Fig. 2. Note that the concentrations of the first sample were initially above zero because a few minutes were needed to collect the first sample for analysis. The aqueous concentrations of the solutes in the eluent increased very fast at the beginning

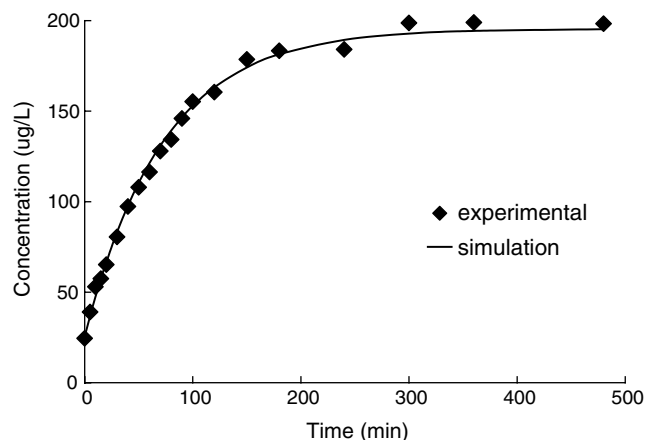


**Fig. 2.** Simulation of analytical solution versus measured concentrations of simple model NAPL ( $k_i = 7.8 \times 10^{-4}$  cm/s, RRSS is 0.02)

of the experiment. This was also the case for the multicomponent NAPL system (see the section “Multicomponent NAPL” below). The fitted mass transfer coefficient  $k_i$  varied between 3 and  $12 \times 10^{-4}$  cm s<sup>-1</sup> for each of the test runs under different conditions. Fitted values for  $k_i$  of phenanthrene matched well with the published data listed in Table 2, but they were consistently in the higher end of the range (Alshafie and Ghoshal 2004; Ghoshal et al. 2004; Ghoshal et al. 1996; Mukherji et al. 1997; Ortiz et al. 1999; Schlupe et al. 2001). The reason for the relatively high value of  $k$  might be that the model NAPL did not contain high-molecular weight hydrocarbons (i.e., asphaltene and resin).

### Multicomponent NAPL

The elution profiles of solutes in the multicomponent NAPL–water system are shown in Fig. 3. The aqueous phase concentrations of phenol and m-cresol reached the maxima at 100 and 200 min, respectively, then decreased either rapidly (phenol) or

**Table 2.** Published Data of Mass Transfer Coefficients ( $10^{-4}$  cm/s)

NAPLs	Naphthalene	Phenanthrene	Benzene	Phenol
Diesel <sup>a</sup>	3.4	3.2	3.9	3.9
Cresote <sup>b</sup>	4–6			
Crude oil <sup>c</sup>	7–12		6–11	6–11
Gasoline <sup>c,d</sup>	11.7		6.7	6.7
Coal tar <sup>e</sup>	2.44–3.05			
Coal tar <sup>f</sup>	0.78	0.62		0.38
Petrolatum <sup>g</sup>	6	7		
Model NAPL <sup>h,i</sup>	8.5–14.2			
Model NAPL <sup>j</sup>	11.0	10.1		
Present study	13.3	10		2.25

<sup>a</sup>Schlupe et al. 2002.

<sup>b</sup>Alshafie and Ghoshal 2004.

<sup>c</sup>Ghoshal et al. 2004.

<sup>d</sup>Gasoline amended with asphaltene and resins.

<sup>e</sup>Ghoshal et al. 1996.

<sup>f</sup>Mahjoub et al. 2000.

<sup>g</sup>Ortiz et al. 1999.

<sup>h</sup>Mukherji et al. 1997.

<sup>i</sup>Toluene solution of naphthalene, 1-methylnaphthalene, 2-ethylnaphthalene, acenaphthene, fluorene, phenanthrene, fluoranthene and pyrene, which was designed to serve as a model for coal tars and creosotes.

<sup>j</sup>Toluene solution of pure component.

slowly (m-cresol). The concentrations of PAHs, phenoxathiin, 1-naphthol, and 2,3-benzofuran increased to their steady state concentrations at different rates and were constant until the end of the experiment. These breakthrough curves are similar to that of phenanthrene in the single-solute model NAPL system (Fig. 2).

To simulate the experimental findings, an ideal solution was assumed at first, i.e., all solutes behaved ideally ( $\gamma_i = \text{constant } \chi_i^n = 1$ ). The numerical solution according to Eqs. (6)–(9) was implemented and the simulation results are shown as lines in Fig. 3. However, the modeled concentrations of most solutes deviated dramatically from the measured data (Fig. 3). Especially for phenol, m-cresol, and 1-naphthol, the modeled concentrations were much lower than those measured in the experiment, although naphthalene and 2, 3-benzofuran obtained higher simulation concentrations.

As a comparison, the variable activity coefficient [Eq. (5)] rather than a constant was employed for all solutes and was simulated by the same numerical solution according to Eqs. (6)–(9). The modeled results are shown in Fig. 4 as lines and the symbols mark the experimental concentrations. The figure illustrates that all concentration profiles match well with the experimental results except for a few points for phenoxathiin and phenanthrene at the beginning of the experiment. This may be because of higher analytical errors associated with their low concentrations at that time period.

The deviation from the ideal behavior (Fig. 3) negates earlier reported successful applications of the simplified Raoult's law in NAPL–water systems (Brown et al. 2005; Cline et al. 1991; Lee et al. 1992; Peters et al. 1997) and corresponds with the observation of Mahjoub (2000). In Mahjoub's studies, phenols were detected as solutes, which is similar to the results in the current system. The disagreement between ideal behavior simulation and experimental results demonstrates a nonideal chemical environment for some solutes in the multicomponent NAPL. This indicates that the activity coefficient should be represented logically as a variable rather than a constant for some solutes in the working system,

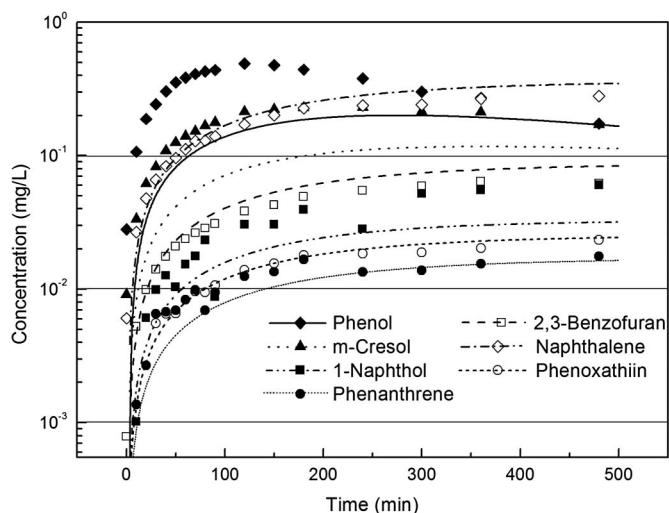


**Fig. 3.** Experimental and simulation concentration profiles for the multicomponent model NAPL with the assumption that all values of  $\gamma_i$  were unities ( $\gamma_i = \text{constant } \chi_i^n = 1$ ); solid lines show the simulated concentrations and the dots represent the experimental data; modeled concentrations of phenols are much lower than those measured, and both naphthalene and 2, 3-benzofuran obtained higher simulation results

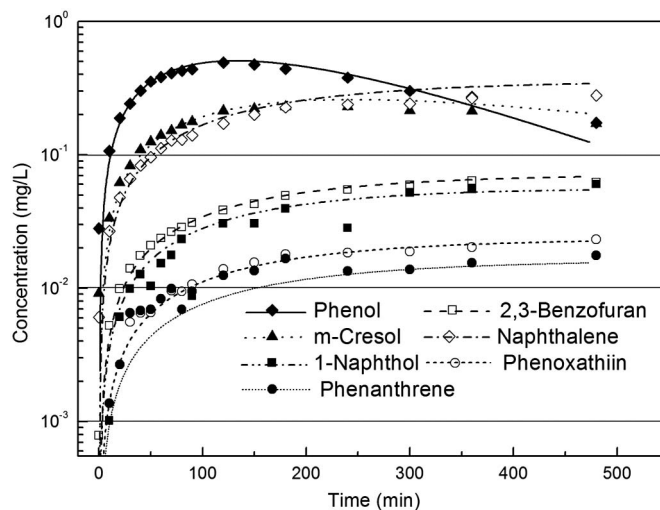


**Fig. 4.** Experimental and simulated ( $\gamma_i = \text{constant } \chi_i^n$ ) concentration profiles for the multicomponent NAPL; solid lines show the simulated concentrations and the dots represent the experimental data

i.e., they should be described as a function of  $\chi_i$ . The functional relationship between  $\chi_i$  and  $\gamma_i$  for some solutes has been proven by experimental data (Ghoshal et al. 1996) and modeling studies (Lee et al. 1998; Lee and Chrysikopoulos 2006).

The values of the estimated parameters  $k$ ,  $\alpha_i$ , and  $n$  obtained using the numerical fitting procedure are listed in Table 3. However, there is no published data of  $k$  available for m-cresol, 1-naphthol, 2,3-benzofuran, or phenoxathiin to compare with the data in this study. The mass transfer coefficient of phenol was the lowest among the solutes. The nonpolar interactions of phenol with the heavier compounds in the NAPL and its hydrogen-bonding characteristics could possibly explain the low mass transfer coefficient. The lower  $k$ -value of phenol is in line with that reported in Mahjoub's study, in which phenol showed the lowest mass transfer coefficient as well (Mahjoub et al. 2000). This could be a result of its low initial concentration combined with its high water solubility. These properties cause a low mass in the NAPL phase after a short leaching time period, which consequently leads to a smaller concentration gradient at the interphase. The  $k$  value of m-cresol was higher than that of 1-naphthol, as expected due to its higher polarity. Similar leaching behavior was found for phenoxathiin and phenanthrene. The  $k$  values of naphthalene and phenanthrene are at the high end of the published data (Table 2). As discussed previously for the single-solute NAPL, the relatively high values may be due to the toluene-based NAPL system. The resistance to mass transfer was thus expected to be lower than

**Table 3.** Simulation Parameters of the Solutes in Complex Model NAPL–Water System

Component	$k_i$ (cm/s) $10^{-4}$	$n$	$\gamma_i$ ( $\chi_i^{n+1}$ )	$\alpha_i$
Phenol	2.25	−0.11	$X^{0.89}$	2.0
m-Cresol	21.7	−0.06	$X^{0.94}$	1.8
1-Naphthol	15.8	−0.03	$X^{0.97}$	1.4
Naphthalene	13.3	0	$X^1$	0.99
Phenanthrene	10	0	$X^1$	0.95
Phenoxathiin	30	0	$X^1$	0.93
2,3-Benzofuran	7.2	−0.02	$X^{0.98}$	0.8

in real NAPL mixtures containing high-molecular weight components and fine mineral particles. The  $k$  value of 2- and 3-ring PHAs (naphthalene and phenanthrene) are very similar and thus were barely distinguishable in this system. This similarity of mass transfer coefficients indicates that for the solvent phase toluene, the difference of molecular structure and physicochemical properties between 2- and 3-ring PAHs does not affect the mass transfer behavior significantly. For solutes with functional groups, their specific properties, e.g., polarity and more diverse intramolecular interactions, obviously contribute to the mass transfer processes in this system. The fitting constant,  $\alpha_i$ , was close to unity for most solutes and changed slightly within the same group of compounds (PAHs, phenols). However, the physical meaning of this parameter remains ambiguous. Clearly, further investigation is needed to obtain additional insight regarding to the mechanisms and physical sense of this constant.

During the leaching process,  $\chi_i$  and  $C_i$  of the compounds changed with the depletion of the solutes. The faster depletion of the more soluble compounds, e.g., phenol and cresol, led to an enrichment of the poorly soluble compounds and subsequently changed the  $\gamma_i$  of these solutes. The change of  $\gamma_i$  is a dynamic process and could be described as a function of  $\chi_i$  [see Eq. (5)]. The parameters could be obtained by fitting the experimental data. Thus, the numerical model provides a convenient method to estimate the  $k$  and  $\gamma_i$  of solutes in complex NAPLs. Fig. 5 shows the trends of  $\gamma_i$  in the model NAPL–water system. The trend lines were obtained by extrapolating the relationship of  $\chi_i$  and  $\gamma_i$  to the points of  $\chi_i = 1$  and  $10^{-7}$ . However, there is no other experimental nor simulation method available to estimate the  $\gamma_i$  of solutes in the current system. Phenoxathiin and PAHs behaved ideally in this system because their molecular properties are very similar to those of the solvent. The  $\gamma_i$  of phenols increased with decreasing mole fractions, which is consistent with the less polar nature of the toluene solvent. Furthermore, for different phenol solutes, values for  $\gamma_i$  increased with increasing polarities in the dilute solutions because a  $-\text{CH}_2-$  group and aromatic ring moiety decrease polarity. 2,3-Benzofuran, as an oxygen-containing heterocyclic compound, falls as expected between phenols and PAHs.

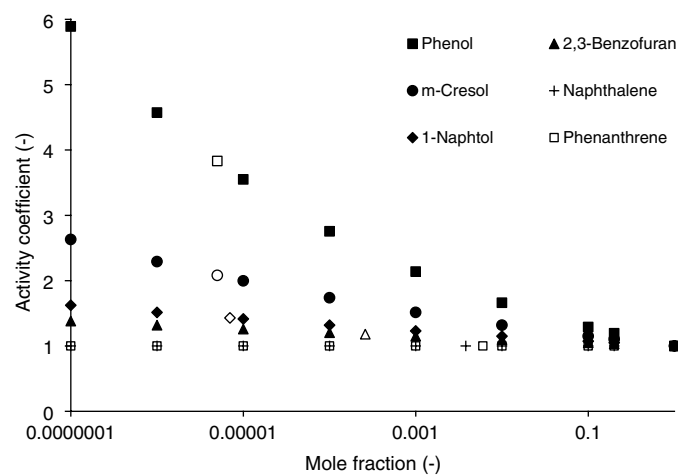


**Fig. 5.** Activity coefficients versus mole fractions according to the numerical simulation results. Phenoxathiin and PAHs behaved ideally (with  $\gamma_i \sim 1$ ); because of overlap, only the values of PAHs are shown; activity coefficients of 2, 3-benzofuran are very small rather than zero; open symbols denote initial mole fractions

## Conclusions

The custom-designed continuously stirred flow-through reactor system can be used to perform mass transfer experiments for NAPL–water systems under different conditions. Raoult’s law with the assumption of the ideal conditions ( $\gamma_i = 1$ ) did not hold for all determined compounds in the multicomponent model NAPL–water system. For the tested multicomponent NAPLs, a numerical model with a variable  $\gamma_i$  was established according to the mass balance equation and a general form of Raoult’s law, in which the activity coefficient varied with system composition and was described as a power function of the mole fraction. The simulated concentration profiles of solutes in the aqueous phase agreed well with the experimental profiles. The mass transfer coefficients of the studied compounds were also determined and the values were then compared to published data if available. The presented numerical model thus provides a convenient tool for quantifying the activity coefficients in complex organic mixtures. The activity coefficients varied with the NAPL composition for phenol, m-cresol, 1-naphthol, and 2,3-benzofuran but remain unity and independent of NAPL composition for naphthalene, phenanthrene, and phenoxathiin. The activity coefficients of aromatic alcohols were positive and decreased with additional  $-\text{CH}_2-$  groups and aromatic rings, as expected. The ideal behavior of PAHs and phenoxathiin is consistent with their similar properties in terms of intermolecular interactions with the solvent toluene.

## Acknowledgments

We gratefully acknowledge financial support by the Deutsche Forschungsgemeinschaft (DFG as part of the research group “transport and reactions in porous media” (HA 3453/6-2)), and thank Noah Stern for language editing, as well as Torsten C. Schmidt and the anonymous reviewers for valuable comments on the manuscript.

## References

- Ahn, B. S., and Lee, W. K. (1990). “Simulation and experimental analysis of mass transfer in a liquid-liquid stirred tank extractor.” *Ind. Eng. Chem. Res.*, 29(9), 1927–1935.
- Alshafie, M., and Ghoshal, S. (2004). “The role of interfacial films in the mass transfer of naphthalene from creosotes to water.” *J. Contam. Hydrol.*, 74(1–4), 283–298.
- Andersen, S. I., del Rio, J. M., Khvostitchenko, D., Shakir, S., and Lira-Galeana, C. (2001). “Interaction and solubilization of water by petroleum asphaltene in organic solution.” *Langmuir*, 17(2), 307–313.
- Barranco, F. T., and Dawson, H. E. (1999). “Influence of aqueous pH on the interfacial properties of coal tar.” *Environ. Sci. Technol.*, 33(10), 1598–1603.
- Benhabib, K., Simonnot, M.-O., and Sardin, M. (2006). “PAHs and organic matter partitioning and mass transfer from coal tar particles to water.” *Environ. Sci. Technol.*, 40(19), 6038–6043.
- Broholm, M. M., Christophersen, M., Maier, U., Stenby, E. H., Höhener, P., and Kjeldsen, P. (2005). “Compositional evolution of the emplaced fuel source in the vadose zone field experiment at airbase Vaerlose, Denmark.” *Environ. Sci. Technol.*, 39(21), 8251–8263.
- Brown, D. G., Gupta, L., Moo-Young, H. K., and Coleman, A. J. (2005). “Raoult’s law-based method for determination of coal tar average molecular weight.” *Environ. Toxicol. Chem.*, 24(8), 1886–1892.
- Brusseau, M. L., Hu, Q., and Srivastava, R. (1997). “Using flow interruption to identify factors causing nonideal contaminant transport.” *J. Contam. Hydrol.*, 24(3–4), 205–219.
- Cho, J., Annable, M. D., and Rao, P. S. C. (2005). “Measured mass transfer coefficients in porous media using specific interfacial area.” *Environ. Sci. Technol.*, 39(20), 7883–7888.

- Chrysikopoulos, C. V., and Lee, K. Y. (1998). "Contaminant transport resulting from multicomponent nonaqueous phase liquid pool dissolution in three-dimensional subsurface formations." *J. Contam. Hydrol.*, 31(1–2), 1–21.
- Chrysikopoulos, C. V., and Kim, T.-J. (2000). "Local mass transfer correlations for nonaqueous phase liquid pool dissolution in saturated porous media." *Transp. Porous Media*, 38(1–2), 167–187.
- Chrysikopoulos, C. V., Hsuan, P.-Y., Fyrrillas, M. M., and Lee, K. Y. (2003). "Mass transfer coefficient and concentration boundary layer thickness for a dissolving NAPL pool in porous media." *J. Hazard. Mater.*, 97(1–3), 245–255.
- Cline, P. V., Delfino, J. J., and Rao, P. S. C. (1991). "Partitioning of aromatic constituents into water from gasoline and other complex solvent mixtures." *Environ. Sci. Technol.*, 25(5), 914–920.
- Eberhardt, C. G. P. (2002). "Time scales of organic contaminant dissolution from complex source zones: coal tar pools vs. blobs." *J. Contam. Hydrol.*, 59(1–2), 45–66.
- Ghoshal, S., and Luthy, R. G. (1998). "Biodegradation kinetics of naphthalene in nonaqueous phase liquid-water mixed batch systems: Comparison of model predictions and experimental results." *Biotechnol. Bioeng.*, 57(3), 356–366.
- Ghoshal, S., Pasion, C., and Alshafie, M. (2004). "Reduction of benzene and naphthalene mass transfer from crude oils by aging-induced interfacial films." *Environ. Sci. Technol.*, 38(7), 2102–2110.
- Ghoshal, S., Ramaswami, A., and Luthy, R. G. (1996). "Biodegradation of naphthalene from coal tar and heptamethylnonane in mixed batch systems." *Environ. Sci. Technol.*, 30(4), 1282–1291.
- Heyse, E., Augustijn, D., Rao, P. S. C., and Delfino, J. J. (2002). "Nonaqueous phase liquid dissolution and soil organic matter sorption in porous media: review of system similarities." *Crit. Rev. Env. Sci. Technol.*, 32(4), 337–397.
- Jeribi, M., Almir-Assad, B., Langevin, D., Henaut, I., and Argillier, J. F. (2002). "Adsorption kinetics of asphaltenes at liquid interfaces." *J. Colloid Interface Sci.*, 256(2), 268–272.
- Khachikian, C., and Harmon, T. C. (2000). "Nonaqueous phase liquid dissolution in porous media: Current state of knowledge and research needs." *Transp. Porous Media*, 38(1–2), 3–28.
- Kim, T.-J., and Chrysikopoulos, C. V. (1999). "Mass transfer correlations for nonaqueous phase liquid pool dissolution in saturated porous media." *Water Resour. Res.*, 35(2), 449–459.
- Lane, W. F., and Loehr, R. C. (1992). "Estimating the equilibrium aqueous concentrations of polynuclear aromatic hydrocarbons in complex mixtures." *Environ. Sci. Technol.*, 26(5), 983–990.
- Lee, C. M., Meyers, S. L., Wright, C. L., Coates, J. T., Haskell, P. A., and Falta, R. W. (1998). "NAPL compositional changes influence partitioning coefficients." *Environ. Sci. Technol.*, 32(22), 3574–3578.
- Lee, K. Y. (2004). "Modeling long-term transport of contaminants resulting from dissolution of a coal tar pool in saturated porous media." *J. Environ. Eng.*, 130(12), 1507–1513.
- Lee, K. Y., and Chrysikopoulos, C. V. (2006). "Dissolution of a multicomponent DNAPL pool in an experimental aquifer." *J. Hazard. Mater.*, 128(2–3), 218–226.
- Lee, K. Y., Khinast, J., Kim, J.-H. (2007). "Numerical modeling of contaminant transport resulting from dissolution of a coal tar pool in an experimental aquifer." *Hydrogeol. J.*, 15(4), 705–714.
- Lee, L. S., Rao, P. S. C., and Okuda, I. (1992). "Equilibrium partitioning of polycyclic aromatic hydrocarbons from coal tar into water." *Environ. Sci. Technol.*, 26(11), 2110–2115.
- Liu, L., Endo, S., Eberhardt, C., Grathwohl, P., and Schmidt, T. C. (2009). "Partition behavior of polycyclic aromatic hydrocarbons between aged coal tar and water." *Environ. Toxicol. Chem.*, 28(8), 1578–1584.
- Luthy, R. G. et al. (1994). "Remediating tar-contaminated soils at manufactured gas plant sites." *Environ. Sci. Technol.*, 28(6), 266A–276A.
- Luthy, R. G., Ramaswami, A., Ghoshal, S., and Merkel, W. (1993). "Interfacial films in coal tar nonaqueous-phase liquid-water systems." *Environ. Sci. Technol.*, 27(13), 2914–2918.
- Mahjoub, B., Jayr, E., Bayard, R., and Gourdon, R. (2000). "Phase partition of organic pollutants between coal tar and water under variable experimental conditions." *Water Res.*, 34(14), 3551–3560.
- Mukherji, S., Peters, C. A., and Weber, W. J., Jr. (1997). "Mass transfer of polynuclear aromatic hydrocarbons from complex DNAPL mixtures." *Environ. Sci. Technol.*, 31(2), 416–423.
- Nelson, E. C., Ghoshal, S., Edwards, J. C., Marsh, G. X., and Luthy, R. G. (1996). "Chemical characterization of coal tar-water interfacial films." *Environ. Sci. Technol.*, 30(3), 1014–1022.
- Ortiz, E., Kraatz, M., and Luthy, R. G. (1999). "Organic phase resistance to dissolution of polycyclic aromatic hydrocarbon compounds." *Environ. Sci. Technol.*, 33(2), 235–242.
- Peters, C. A., Knightes, C. D., and Brown, D. G. (1999). "Long-term composition dynamics of PAH-containing NAPLs and implications for risk assessment." *Environ. Sci. Technol.*, 33(24), 4499–4507.
- Peters, C. A., Mukherji, S., Knightes, C. D., and Weber, W. J., Jr. (1997). "Phase stability of multicomponent NAPLs containing PAHs." *Environ. Sci. Technol.*, 31(9), 2540–2546.
- Powers, S. E., Abriola, L. M., and Weber, W. J., Jr. (1992). "An experimental investigation of nonaqueous phase liquid dissolution in saturated subsurface systems: Steady state mass transfer rates." *Water Resour. Res.*, 28(10), 2691–2705.
- Powers, S. E., Loureiro, C. O., Abriola, L. M., and Weber, W. J., Jr. (1991). "Theoretical study of the significance of nonequilibrium dissolution of nonaqueous phase liquids in subsurface systems." *Water Resour. Res.*, 27(4), 463–477.
- Ramaswami, A., Ghoshal, S., and Luthy, R. G. (1997). "Mass transfer and bioavailability of PAH compounds in coal tar NAPL-slurry systems. 2. Experimental evaluations." *Environ. Sci. Technol.*, 31(8), 2268–2276.
- Ramaswami, A., and Luthy, R. G. (1997). "Mass transfer and bioavailability of PAH compounds in coal tar NAPL-slurry systems. 1. Model development." *Environ. Sci. Technol.*, 31(8), 2260–2267.
- Schluep, M., Galli, R., Imboden, D. M., and Zeyer, J. (2002). "Dynamic equilibrium dissolution of complex nonaqueous phase liquid mixtures into the aqueous phase." *Environ. Toxicol. Chem.*, 21(7), 1350–1358.
- Schluep, M., Imboden, D. M., Galli, R., and Zeyer, J. (2001). "Mechanisms affecting the dissolution of nonaqueous phase liquids into the aqueous phase in slow-stirring batch systems." *Environ. Toxicol. Chem.*, 20(3), 459–466.
- Sullivan, A. P., and Kilpatrick, P. K. (2002). "The effects of inorganic solid particles on water and crude oil emulsion stability." *Ind. Eng. Chem. Res.*, 41(14), 3389–3404.
- Tiruta-Barna, L., Mahjoub, B., Faure, L., Hanna, K., Bayard, R., and Gourdon, R. (2006). "Assessment of the multi-compound non-equilibrium dissolution behaviour of a coal tar containing PAHs and phenols into water." *J. Hazard. Mater.*, 132(2–3), 277–286.
- Zheng, J. Z., and Powers, S. E. (2003). "Identifying the effect of polar constituents in coal-derived NAPLs on interfacial tension." *Environ. Sci. Technol.*, 37(14), 3090–3094.